GeoVirtual 2020 September 14-16
Resilience and Innovation
CGS.ca

Numerical 3D model supporting decision of waterproofing or installing a drainage system attenuating structures damage risks

Moussa Kfoury & Sylvain Roy
Englobe Corp., Laval, Québec, Canada

ABSTRACT
The development of a new project is happening on a complex site. The overburden soil stratigraphy is heterogeneous and sensitive to settlement. Projected structures are an underground station, vertical shafts, main cavern and a tunnel. Associated transit structures are also planned to ensure connection with the Express Network Metropolitan of Montreal (REM). Shallower structures such as multi-level car parks and bus facilities are also planned. Authors have assessed the potential damages, and risks related to the lowering of water table. Such water level drop is caused by pumping operations. This paper presents the different phases of building the numerical 3D model. Then, it highlights main parameters that would impact the predictive hydrogeological results. After that, it describes the evolution of the infiltration rate during construction sequences. Moreover, it assesses the draw down of water table following a decision to waterproof or not. Finally, it expresses monitoring approaches to mitigate the risk of potential damage.

RÉSUMÉ
Sur un site de stratigraphie complexe sur lequel reposent plusieurs installations sensibles aux tassements de sol, de nombreuses structures seraient construites, c.-à-d. une station souterraine, des noyaux verticaux, une caverne, un tunnel et des structures de transit permettant la communication avec le Réseau Express Métropolitain de Montréal (REM). Des structures moins profondes sont également prévues dans le plan de développement du site. Les auteurs ont effectué une évaluation des conséquences que peut avoir le rabattement du niveau d'eau souterraine et des dommages potentiels dus aux opérations de pompage.
Cet article présente les étapes de construction du modèle numérique, discute des paramètres qui influencent les résultats hydrogéologiques prédictifs, expose l'évolution du débit d'écoulement des eaux souterraines pour une séquence de construction, évalue le rabattement du niveau d'eau souterraine faisant suite à une décision d'imperméabilisation ou de drainage et formule des méthodes de suivi permettant d'intervenir pour atténuer le risque de dommages potentiels.

1 INTRODUCTION

The development of a new project on a complex site is going on. The overburden soil stratigraphy is heterogeneous and sensitive to settlement. Native soil is composed partly by Leda clay from Champlain's sea episode, a sand deposit from early St. Lawrence river episode and a till from Malone glacial episode. An underground station, vertical shafts, main cavern, tunnel, flare and associated transit structures are planned. Underground structures will be carried out by drill and blast within the bedrock. The calculated volume of rock excavation is about 67,000 m^3. Shallower structures must be built on superficial deposits. A temporary soldier pile wall and a secant pile wall are proposed to hold soil at critical places. The projected structures will connect the existing facilities to the Express Network Metropolitan of Montreal (REM: *Réseau Électrique de Montréal*). The REM is a major project for the collective transport of light rail trains in Montreal and surrounding area. Besides, several shallower structures such as multi-level car parks and bus facilities will be constructed on glacial till. A soldier pile is a common retaining wall strategy considered in the project.

During excavation and construction phases, groundwater inflow will likely happen. The drawdown of water table can have detrimental effects to soil settlements. It can increase risks of potential damage on existing installations. The reason is that when groundwater is withdrawn, water table level drops, pore water pressure reduces, effective stress increases which lead to start the consolidation of a cohesive soil.

It becomes valuable to know the type of existing foundations, the soil underneath and the lowering level of water table. The combination of all those factors results on a vertical settlement of the soil. The progress of settlement depends on the permeability of the soil, the length of the drainage path and the compressibility of the soil. For instance, permeability of a clayey soil is lower than permeability of sandy soils. So, the dissipation of pore pressure in a clayey soil is slower than the one in sandy deposits. In a heterogeneous overburden soil as encountered in this site, the settlement will occur in a not uniform way. Besides, the settlement initiated by the drawdown of the water table is evaluated to happen over a period up to 20 years.

To assess groundwater infiltration rate, it is important to consider construction sequences. Excavation techniques and waterproofing operations must be look at. For instance, if pumping rate is higher than recharge rate of aquifers, the water table is lowered. The area of influence is extended around pumping stations. It depends on heterogeneity of overburden and bedrock. It also depends on fracture clusters having an impact on horizontal and vertical conductivity.

Authors have proceeded by collecting data from existing studies done since 1955. It allowed to build a detailed 3D numerical model using available information. It helped to assess the potential damages and risks related to the draw down of groundwater level.

This paper presents the different phases of building the numerical 3D model. Then, it highlights main parameters that would impact the predictive hydrogeological results. So, it describes the evolution of the groundwater infiltration rate during construction sequences. Moreover, it assesses the draw down of water table further to a decision to waterproof or not. Finally, it expresses monitoring approaches to mitigate the risk of potential damage.

This assessment is made for the construction period (transient state) and for the next operation period (steady state). The 3D numerical model has helped with the decision on waterproofing or not for a many projected structure. The principal goal is to build new structures by avoid a potential damage risk on existing installations.

2 REGIONAL GEOLOGY

The Island of Montreal has been glaciated. It has resulted in the deposition of very dense boulder till on the surface of the bedrock over most of the island. The topography of the site in study is flat and can be related to next inter-glacial or post-glacial deposits. According to Prest et al. (1982), local geology of the site includes marine deposits belonging to Champlain sea episode, sand deposits belonging to the Early Lawrence river episode and glacial till belonging to Malone glacial episode. Overburden soil overlay bedrock. It consists of the Tétreauville formation covering the Montréal Formation. Both belongs to the Paleozoic Ordovician Trenton Group.

3 DATA COLLECTION

Authors have collected and analyzed data from about 260 studies done for this site since 1955. Stratigraphy of the site has been built using information from 1,700 boreholes. Many seismic lines helped to point the top of bedrock. Measurements done on site and in the laboratory were important to build a 3D hydrogeological numerical model. The 3D model was history matched with available data.

3.1 Ground surface

The studied site covers an area of about 25 km2. The ground surface is tilting toward the south with an elevation decreasing from 39 m to 21 m. The surface of the ground was built using aerial Lidar survey done in 2015 and altimeter data done on some parts of the site. Aerial Lidar was collected from public data published on the site of the City of Montreal. The Canadian Geodetic Vertical Datum CGVD28 was considered for altimeters referencing.

3.2 Site geology

Geotechnical investigations have allowed building internal stratigraphy using observations from boreholes. Native soil is composed by a thick Leda clay overlying till deposits in the western and southern part of the site. In the northern and eastern part, a thin Leda clay overlying till is observed. A sand body channelling from north toward the south in the western side of the site and covering a thin layer of Leda clay is captured.

Beyond the northern limit of the site, Leda clay deposit seems to disappear. Whereas, sand deposits and glacial till still appear according to Prest et al. (1982). The northern part of the site is the main watershed recharging both superficial and deeper groundwater aquifers.

Composition of glacial till deposits seems to be variable in the site area. A high concentration of cobbles and boulders in the lower part of the till is noticed. These cobbles and boulders are limestone but occasionally metamorphic or igneous. The upper part of the till is composed of a mixture of sand, gravel and silt.

The bedrock belongs to the Paleozoic Ordovician Trenton group. It consists of the Tétreauville formation overlying the Montréal formation. The Tétreauville Formation consists of micritic limestone with a shale content ranging between 25% and 75%. The contact between limestone and shale is planar. The Montréal Formation consists of limestone containing fossils with a shale content ranging between 30% and 60%. The contact between limestone and shale is undulated.

3.3 Groundwater

812 measurements of water table level have been collected from many piezometers installed over the entire site. Those piezometers have targeted sand deposits, Leda clay, till deposits and bedrock. Figure 1 illustrates the outcomes of groundwater level measurements collected since 1959. The average value of groundwater level is dropping by almost 3m since 1959 to present. The lowering of groundwater level was caused by urbanism developments and by pumping

stations. Urbanism development has involved the following consequences:

- Decrease of aquifers recharge due to waterproofing of ground surface
- Excessive pumping around infrastructure built in the nearby area of the site that lower groundwater table level
- planting of rapid-growing trees that need a much higher need of water absorption than traditional trees
- Temporary pumping operations during excavation and construction phases that lower groundwater level.

The topography of the site and his watershed is sloping from the north toward the south. Groundwater flow is following also the same direction from north to south. The infiltration of water within watershed and site area is recharging local aquifers. In the watershed at the northern part of the site, clay formation is not present. Vertical hydraulic gradient between sand and till aquifers is small with a downward flow. Both aquifers are unconfined at this location. Leda Clay formation becomes more present by approaching the site of study. Hydraulic pressure regimes become different between sand and till aquifers. A higher vertical gradient is noticed. Sand aquifer remains unconfined while till aquifer becomes confined in the studied site area. In the other hand and due to the glacial event, the upper part of the bedrock is often weathered. It helped to equilibrate hydraulic regimes between till and bedrock aquifers at some locations.

The vertical hydraulic gradient is computed between two points. It corresponds to the ration of hydraulic head variation to the vertical distance. In the context of this paper, a positive value means a downward flow while a negative value means an upward flow. Few piezometers with two standpipes have targeted different stratigraphy. It allowed computing vertical hydraulic gradient which is ranging from:

- 0.399 to 0.685 between sand and Leda clay soils
- 0.012 to 0.331 between Leda clay and till deposits
- 0.191 to 0.287 between sand and till deposits
- -0.035 to 0.055 between till deposits and bedrock
- -0.242 and 0.138 between upper and lower part of bedrock nearby existing pumping stations.

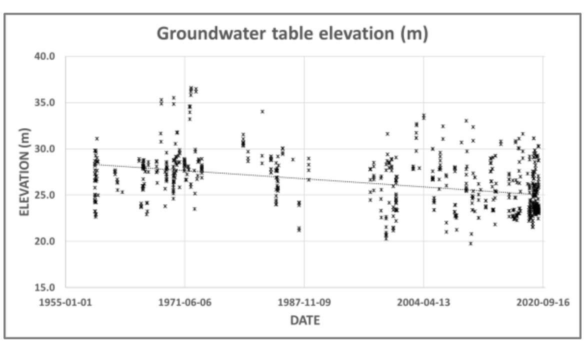

Figure 1. Groundwater elevation since 1959 to present 1999)

Vertical hydraulic gradient is generally confirming a downward vertical flow. Some exceptions are captured between till deposits and bedrock near existing pumping stations. It is related to the recharge of the aquifer and to the vertical hydraulic conductivity.

3.4 Hydraulic conductivity

185 measurements of hydraulic conductivity performed on site were collected from existing studies. Those measurements have targeted sand, clay and till deposits as the bedrock. Figure 2 illustrates the measurement of hydraulic conductivity for each soil deposits and for the bedrock. Packer testing (or Lugeon testing) was used in the bedrock to determine hydraulic conductivity. None of those packers testing was performed in weathered fractured rock. In the cohesive deposits, the measured hydraulic conductivity is varying between 3.7 x 10^{-9} m/s and 9.9 x10^{-6}. In clay deposits, hydraulic conductivity increases as silt percentage increases in this deposit. In the granular deposits, the measured hydraulic conductivity is ranging between 2.5 x10^{-8} and 5.7 x 10^{-5} m/s. In a granular deposit, hydraulic conductivity decreases as long as fine minerals increases in this deposit. In the till deposits, the measured hydraulic conductivity is varying between 7.7 x10^{-8} and 3.7 x 10^{-4} m/s. The hydraulic conductivity is related to grain size and to the percentage of fine minerals. Finally, measured hydraulic conductivity of bedrock is ranging between 5.6 x10^{-9} and 1.4 x 10^{-4} m/s. The highest values of hydraulic conductivity in bedrock indicates the presence of open fractures.

All hydraulic conductivity measurements were done in fully saturated soils. In unsaturated zone above the free surface, hydraulic conductivity will drop with pore pressure (Bouwer 1964, Freeze 1971, Desai et al. 1983). Those measurements were used to generate 3D spatial distribution of hydraulic conductivity.

Groundwater infiltration rate is proportional to hydraulic conductivity and to hydraulic gradient.

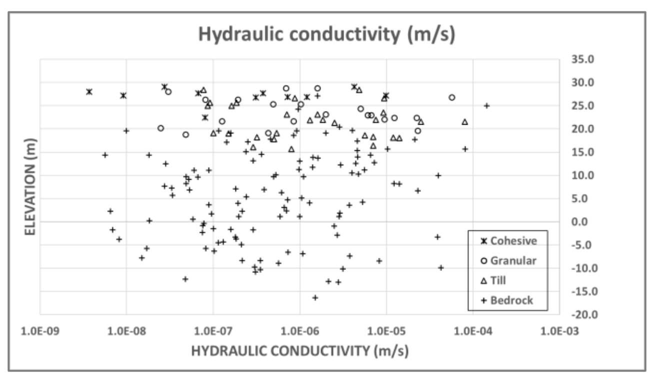

Figure 2. Hydraulic conductivity measured on site

3.5 Moisture content

Existing studies have allowed collecting almost 910 moisture content measurements. It has been performed in the laboratory on soil samples collected from sand, clay and till deposits since 1955. The outcome is presented in figure 3. It is noted that a unique correlation is not possible. It is related to the decline of water table level and to the heterogeneity of soil types. In unsaturated zone, moisture content is held between soil grains under surface-tension forces also known by capillary pressure (Liakopoulos 1965a). However, in a fully saturated zone, the soil porosity is filled by water.

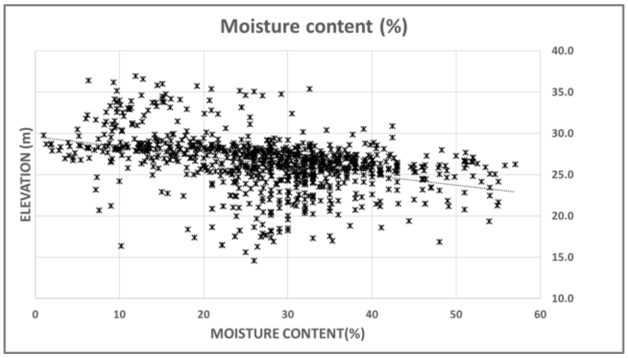

Figure 3. Profile of moisture content versus depth

3.6 Atterberg limits

The Atterberg limits provide a useful sign of the properties of cohesive soils. Almost 903 measurements were available from existing studies. Figure 4 illustrates a histogram for plastic limits, liquid limit and plasticity index. Table 1 indicates the average and standard deviation of Atterberg limits.

Table 1. Atterberg limits

Properties	Average	Standard deviation
Plastic limit	20	4.9
Liquid limit	37	13.1
Plasticity index	17	9.7
Liquidity index	0.5	0.3

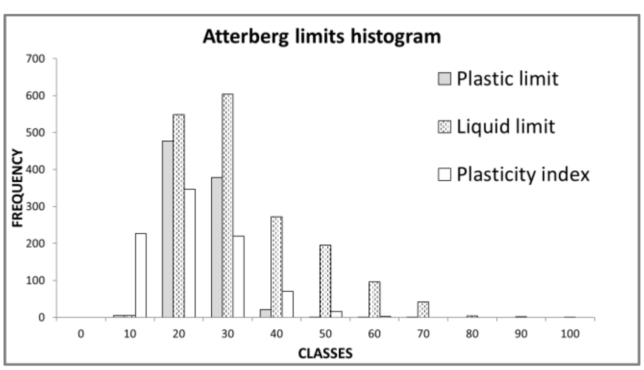

Figure 4. Atterberg limits histogram

According to Burmister (1949) and Bergaya et al. (2013), cohesive soil with a plasticity index (PI) between:

- 5 and 10 is characterized by a low plasticity
- 10 and 20 is classified by a medium plasticity
- 20 and 40 is classed with high plasticity
- Beyond 40 is judged with very high plasticity.

3.7 Undrained shear strength

59 measurements of undisturbed shear strength and 13 measurements of remoulded shear strength were executed in Leda Clay deposit. 13 measurements are obtained using vane shear tests on site. 46 measurements are acquired using cone penetrometer tests in the laboratory. The outcome is presented in the figure 5. The average and standard deviation of cohesive soil sensitivity are respectively 9.3 and 5.9. It means that the cohesive soil is classed sensitive to extra sensitive.

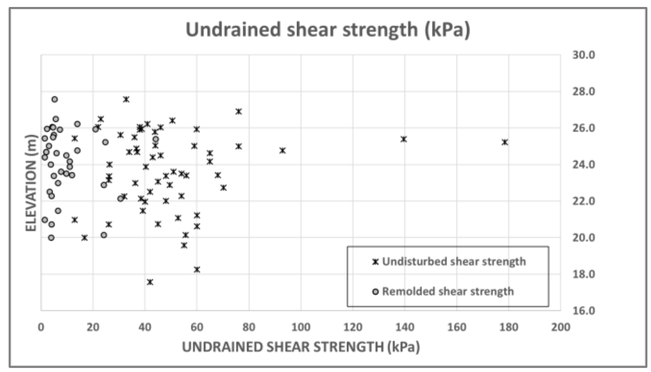

Figure 5. Undisturbed and remolded shear strength

3.8 Oedometer consolidation test

45 oedometer consolidation tests were collected from existing studies. Oedometer is a classical and practical test executed in the laboratory to get parameters for consolidation. It helps to assess settlement under consolidation. It also allows assessing the stress history of soils. The outcome is illustrated in figure 6. Table 2 indicates the average and standard deviation of the outcome from oedometer consolidation test.

Table 2. Average and standard deviation of computed parameters from oedometer test

Properties	Average	Standard deviation
Void ratio	0.97	0.26
Recompression index	0.036	0.012
Compression index	0.382	0.247
Preconsolidation pressure	197	73
Field effective overburden pressure	82	24
Overconsolidation ratio	2.7	1.1

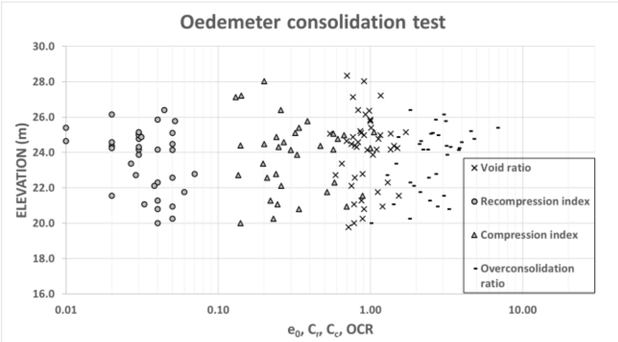

Figure 6. Oedometer consolidation test outcome

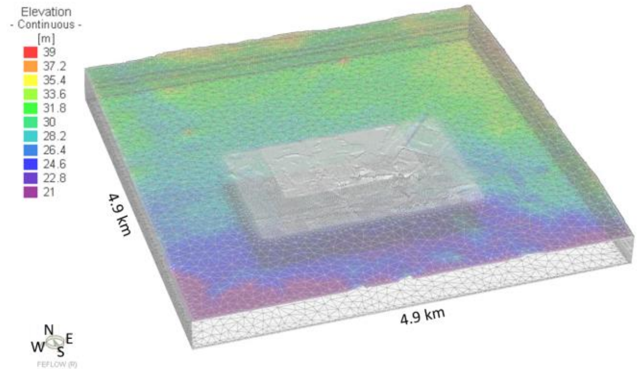

Figure 7. Geometry and mesh of 3D numerical model

4 OBJECTIVES

The first goal is to support the decision of waterproofing or not of new structures. The second aim is to assess the potential damages and risks related to groundwater lowering under pumping operations. To reach targets, it requires a teamwork involving hydrogeologist, geotechnical and structural engineers. This process will establish alert flags for water table level and for soil settlement. The settlement must respect structures acceptance criteria.

A 3D numerical model was built using Feflow software, a product of DHI, to predict groundwater flow and drawdown. Several 2D sections at a key location were taken and analyzed in SIGMA/W software, a product of GEOSLOPE, to assess the soil settlement. This paper does not address the structural acceptance criteria assessed by structural team.

5 HYDROGEOLOGICAL NUMERICAL MODEL

Feflow 7.2 was used to build a numerical 3D model. It aimed to assess variation of groundwater levels. It also purposed to estimate temporary and permanent water infiltration flow rate.

5.1 Geometry

A 3D model was prepared using Civil 3D, a powerful software of Autodesk. It integrates Lidar, altimeter surveys, bedrock top from both seismic lines and from boreholes. Triangle model was used to interpolate and extrapolate elevation within the area of the model. Geometry has been imported into Feflow and then validated to ensure the integrity of imported information. The model has been meshed with almost 1.8 million cells. Around existing installations and projected structures, the mesh cell edge size is around 7m. It becomes larger about 15m in the surrounding area and reaching around 100m in the external part of the model. Figure 7 presents the 3D meshed model with the elevation of ground level.

5.2 Hydraulic properties

Available hydraulic conductivity measurements from existing studies were done as follows:

- 21 measurements in sand deposits
- 11 measurements in Leda clay deposit
- 30 measurements in till deposit
- 123 measurements in bedrock done mainly in a limited area of interest for the project.

The exact location of those tests was used in the model to generate several aerial mappings of hydraulic conductivity. Several algorithms available in Feflow were considered. Available algorithm is inverse distance, kriging, Akima, Neighbourhood relationship and Point in elements. At the four edges of model area an average value of the measured hydraulic conductivity was considered. It allows controlling extrapolated data for each stratigraphy unit. Figure 8 illustrates a typical outcome of hydraulic conductivity maps. The aerial mapping view for hydraulic conductivity in till is on left side and in the bedrock is on right side. The whole studied area is about 4.9km x 4.9km.

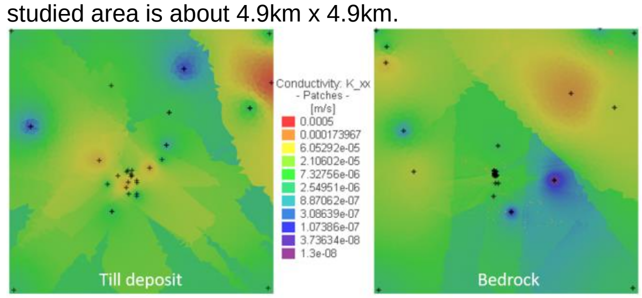

Figure 8. Hydraulic conductivity mapping in till deposits (left side), in the bedrock (right side) and location of measurements ("+" sign)

5.3 Fractured bedrock

Fractured bedrock was encountered at 131 boreholes. In figure 9, horizontal axis embodies boreholes that have encountered fractured rock. The vertical axis represents elevation of top and bottom parts of fractured rock for each of these boreholes. The name of boreholes was not shown due to privacy consideration. These fractured windows were placed aerially at borehole emplacements and in a vertical layer honoring their elevation. The figure 10 illustrates borehole location that has encountered fractured rock at top of the bedrock ("+" sign at left side). The network of fractures depends on spatial inter-connectivity between those features. Sometimes, a dedicated geophysical investigation will constitute a driver for fractures networks. Due to lack of such driver, several scenarios were considered. In the history match process, adjacent fracture clusters were connected within a radius of 10m, 15m, 20m and 25m.

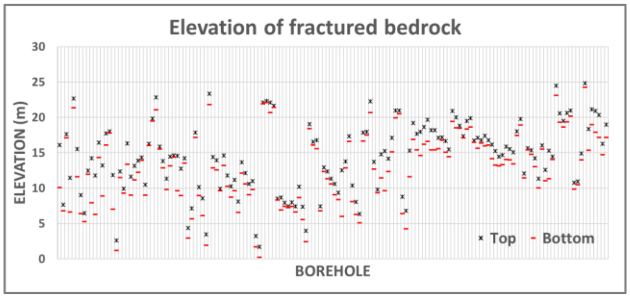

Figure 9. Elevation of top and bottom windows of fractured rock for each one of 131 boreholes

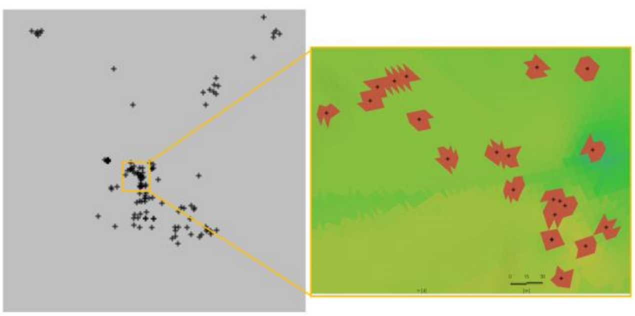

Figure 10. Fractured rock at the top of the bedrock placed at borehole location ("+" sign at left side) and a focus window showing inter-connectivity scenario of fracture networks (orange shape at the right side)

5.4 Hydrologic boundaries

The hydrologic boundaries in the model corresponds to the areas from which water is entering and leaving. The site is bounded by a river to the south with an averaged elevation of the water surface at about 21m for the last 100 years. The upper boundary of the northern part is modelled to receive recharge from precipitation. West, east and north sides are modelled with a flux boundary condition with no inflow.

5.5 Precipitation and recharge

Precipitation is the principal source of water recharge into the aquifer. Recharge rate is computed considering several factors. Precipitation, evapotranspiration and the capacity of soils to store water are considered. Also, the topography of the site is an important factor to estimate the recharge rate. Table 3 indicates the yearly averaged temperature and yearly total precipitation. Data have been collected from a weather station close to the studied site. A hydrological balance was done considering all those factors. The recharge of the aquifer is evaluated to vary between 70 and 105mm/year. This parameter is highly impacting the match of historical data. A value of 87mm/year offers the best model matching measured hydraulic heads and pumping rates.

Table 3. Temperature and precipitation at the site

Characteristics (%)	Temperature[1]	Precipitation[2]
2016	8.1	1037.8
2017	7.6	1252.3
2018	7.3	1046.4
2019	5.8	1196.7

[1]yearly average value of temperature in degrees Celsius
[2]total yearly precipitation in millimeters
Note: data collected from https://climate.weather.gc.ca/

5.6 Groundwater withdrawals

Two facilities were completely built in 2005 and in 2015. Permanent pumping systems were installed under the slab on grades. The averaged yearly pumping rate was collected for a period of 7 years as illustrated in figure 11. The averaged value of pumping rate is about 8.6l/s and 10.2l/s for installation #1 and installation #2. For installation #1, the low pumping rate value reported in the year number 4 is related to clogged pipes issues.

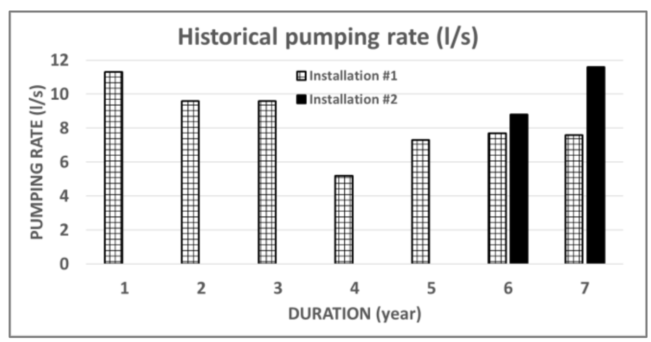

Figure 11. Historical yearly averaged pumping rates.

6 HISTORY MATCHING AND SENSITIVITY

History matching process for calibration of 3D numerical model was based on water levels measured at a key piezometer. It also founded on pumping rates reported from the two existing installations. The observations were selected based on quality of data. It provides a reasonable spatial distribution over the site area of water levels (Hölting et al. 2019 and HIS et al. 1994). History matching is an iterative process where parameters representing model properties are adjusted. The purpose is to tune the model in response to the correspondence between observations and computed model outputs. Four types of parameters were considered in the history matching process:

- recharge from precipitation
- spatial distribution of hydraulic conductivity
- vertical anisotropy of hydraulic conductivity
- inter-connectivity of fracture clusters
- and hydraulic conductivity of fracture clusters

The outcome of the history matching process is a base case or a reference case model that used for prediction scenarios.

6.1 Head observation

Ample water-level observations were available from existing studies. Measured head observation is a valuable information for history matching of the 3D numerical model. It is important to select a representative data with a frequent measurement to ensure a high quality of confidence. 44 wells across the site were selected to calibrate numerical models by matching hydraulic head.

The computed water level from a numerical model was judged by comparing to the Root Mean Squared (RMS) error (Anderson et al. 1992). RMS error is the square root of the sum of the square of the differences between calculated and observed heads divided by the number of observation wells as indicated in Eq. 1.

$$RMS = \sqrt[2]{\frac{1}{n}\sum_{i=1}^{n}(h_m - h_s)^2} \qquad [1]$$

Figure 12 presents computed hydraulic head from the base case model versus observed hydraulic head at 44 piezometers location. RMS of the reference case is 1.08 m.

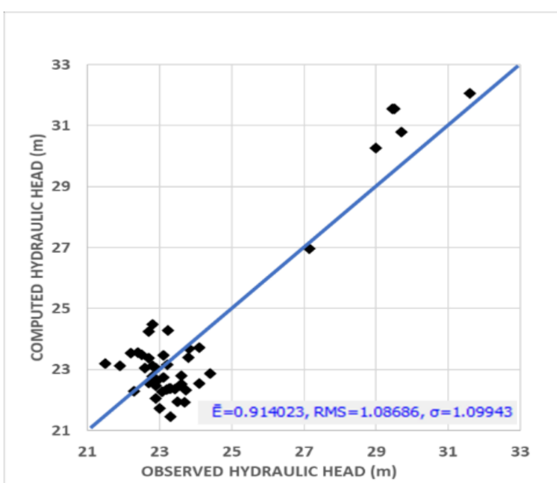

Figure 12. Hydraulic head scatter plot

6.2 Simulated pumping rate

The reference model is estimating a pumping rate of about 9.0 l/s and 9.9 l/s for installation #1 and installation #2. Simulated results are a in a good agreement with reported measurements in section 5.6.

6.3 Sensitivity

The purpose of a sensitivity analysis is to quantify the impact of each parameters on model outcomes. It also allows to check the uncertainty of the calibrated model. Four key parameters presented earlier were stressed to check the size of change in hydraulic heads and in pumping rates. The table 4 presents RMS and pumping rate for the base case and for scenarios where parameters have deviated from the base case.

Table 4. Sensitivity analysis impacting RMS and rate compared to base case

Parameter	RMS (m)	Installation #1 rate (l/s)	Installation #2 rate (l/s)
Recharge[1]	5.89	22.2	16.7
Spatial distribution[2]	3.03	9.7	1.8
Anisotropy[3]	1.26	10.1	10.2
Fractures conductivity and interconnectivity[4]	1.52	10.5	8.8
Base case	**1.08**	**9.0**	**9.9**

[1]recharge of 200 mm/year
[2]example of another spatial distribution of hydraulic conductivity
[3]vertical anisotropy of hydraulic conductivity equal to 1
[4]fractures inter-connectivity within a radius of 20 m & k=10^{-2} m/s

7 GROUNDWATER LOWERING

For a defined sequence of construction, groundwater lowering has been evaluated using the 3D numerical base case. Figure 13 illustrates the lowering level of groundwater after 160 and 560 days since beginning of operations. This scenario does not consider any waterproofing intervention during this lapse of time.

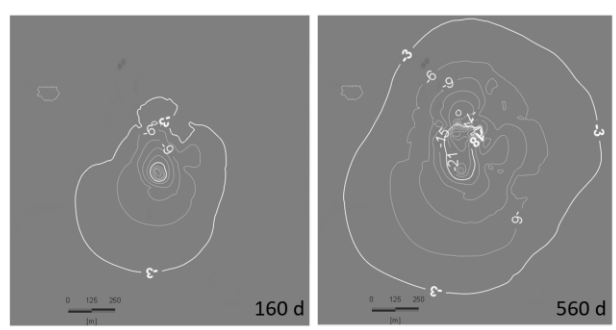

Figure 13. Drawdown of groundwater after 160 days (left side) and 560 days (right side)

8 SETTLEMENT

Groundwater lowering will lead to an extra load on the subsoil layers. It will result in subsidence of the soil and, hence, the structures. Settlement was assessed using SIGMA/W software under all existing installations. Modified Cam-clay model was considered for Leda clay deposit. Figure 14 shows stratigraphy of soil and bedrock. It also illustrates predicted settlement under a typical critical existing installation. Settlement assessment allowed identifying critical installations that need close monitoring.

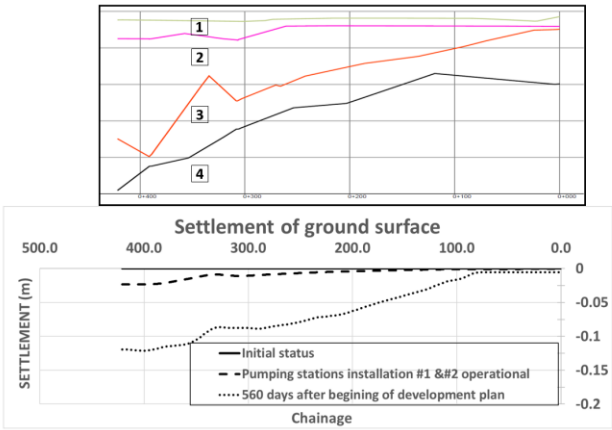

Figure 14. Top: stratigraphy at a cross-section (1: granular, 2: cohesive, 3: till and 4: bedrock). Bottom: drawdown of groundwater levels after the start-up of both pumping station (dashed line) and 560 days after the beginning of the development plan (dotted line)

9 WATERPROOFING AND DAMAGE EVALUATION

Predictive simulation has allowed to identify a weathered zone that intercept the wall of an access shaft. It can lead to a significant water infiltration. A grouting operation was performed by pumping nearly 49,000 litres of hydraulic cement to seal fracture clusters. The remediation job was done before the excavation. A weathered fractured zone on the top of a cavern must also be cured. For sure, it will lead to an elevated water infiltration rate and to a significant lowering of groundwater. Waterproofing operations are projected from the ground surface through dedicated boreholes. It is planned to be done before excavation.

Secant pile wall was also recommended for new structures that are very close to existing installations. Secant pile will be penetrating glacial till and embedded into sound bedrock. Local sealing operations during excavation was recommended to control water infiltration.

Monitoring of water table level and soil movement is on going. It is crucial for ensuring infrastructure integrity. Mitigation actions are also on going to reduce potential damages risk on existing installations.

10 CONCLUSION

A 3D numerical model has been built using Feflow for the evaluation of groundwater lowering. A history matching process has allowed to tune base model honouring water levels and pumping rate observations. SIGMA/W software has been used to assess the soil settlement caused by the lowering of the water table. A 3D civil model helped to integrate geometry and internal stratigraphy of the site by collecting data from more than 260 studies. Ample geotechnical and hydrogeological information have been collected. Those data have been assessed and then integrated into the model. Predictive simulation following operations have allowed identifying critical issues under existing installations. Recommendations have targeted waterproofing of dedicated projected structures. It also aimed to seal defined fractured zones. Besides, a monitoring program to follow groundwater level and soil movement was set up. All those actions were performed to ensure integrity of existing installations.

11 REFERENCES

Prest, V.K. and Keyser, J.H. 1982. *Caractéristiques géologiques et géotechniques des dépôts meubles de l'Île de Montréal et des environs*, Commission géologique du Canada, Étude 75-27.

Bouwer, H. 1964. Unsaturated flow in ground-water hydraulics, *J. Hydraul. Div. Am. Doc. Civ. Engrs 90*, HY5, 121-144.

Freeze, R.A. 1971. Influence of the unsaturated flow domain on seepage through early dams. *Wat. Resour. Res. 7*, No. 4, 929-941.

Desai, C.S. and Li, G.C. 1983. A residual flow procedure and application for free surface flow in porous media. *Adv. Wat. Resour. 6*, 27-35.

Liakopoulos, A.C. 1965b. Variation of the permeability tensor ellipsoid in homogeneous anisotropic soils. *Water Resources Res.*, 1, 135-141.

Burmister, D.M. 1949. Principles and techniques of soil identifications, *Proceedings of Highway Research Board*, 402-433.

Bergaya F. and Lagaly, G. 2013. *Handbook of Clay Science*, Volume 5, 2nd Edition, Elsevier.

Hölting, B. and Coldewey, W. G. 2019. *Hydrogeology*, Springer, Berlin, Germany.

Anderson, M.P. and Woessner, W.W. 1992. Applied groundwater modeling - Simulation of flow and advective transport, *Academic Press*, San Diego, CA, 381.

HIS, J.P., Carter, J.P. and Small, J.C. 1994. Surface subsidence and drawdown of the water table due to pumping, *Géotechnique*, 44, No. 3: 381-396.